New absorption liquids for the removal of CO2 from dilute gas streams using membrane contactors

Kumar, P.S.; Hogendoorn, J.A.; Feron, P.H.M.; Versteeg, G.F.

Published in:
Chemical Engineering Science

DOI:
10.1016/S0009-2509(02)00041-6

PERGAMON

Chemical Engineering Science 57 (2002) 1639–1651

Chemical Engineering Science

www.elsevier.com/locate/ces

New absorption liquids for the removal of CO_2 from dilute gas streams using membrane contactors

P. S. Kumar[a], J. A. Hogendoorn[a], P. H. M. Feron[b], G. F. Versteeg[a,*]

[a] *OOIP Group, Faculty of Chemical Technology, University of Twente, P.O. Box. 217, 7500AE Enschede, The Netherlands*
[b] *TNO Environment, Energy and Process Innovation 7300AH Apeldoorn, The Netherlands*

Abstract

A new absorption liquid based on amino acid salts has been studied for CO_2 removal in membrane gas–liquid contactors. Unlike conventional gas treating solvents like aqueous alkanolamines solutions, the new absorption liquid does not wet polyolefin microporous membranes. The wetting characteristics of aqueous alkanolamines and amino acid salt solutions for a hydrophobic membrane was studied by measuring the surface tension of the liquid and the breakthrough pressure of the liquid into the pores of the membrane. The dependence of the breakthrough pressure on surface tension follows the Laplace–Young equation. The performance of the new absorption liquid in the removal of CO_2 was studied in a single fiber membrane contactor over a wide range of partial pressures of CO_2 in the gas phase and amino acid salt concentrations in the liquid. A numerical model to describe the mass transfer accompanied by multiple chemical reactions occurring during the absorption of CO_2 in the liquid flowing through the hollow fiber was developed. The numerical model gives a good prediction of the CO_2 absorption flux across the membrane for the absorption of CO_2 in the aqueous amino acid salt solutions flowing through the hollow fiber.

Keywords: Absorption; Mass transfer; Membranes; Gas–liquid contactor; Gas separation; Wetting

1. Introduction

Membrane gas–liquid (G–L) contactors make use of a porous polymeric membrane to separate the gas and liquid phase. Ideally, the micro-pores of the membrane should be completely gas filled, to minimize any mass transfer resistance due to the presence of the membrane. Hence, the membranes themselves usually do not offer any selectivity for the gases to be separated; this role is fulfilled by the absorption liquid. Reactive absorption liquids are preferably used above physical absorption liquids as their absorption rate and capacity are generally much better. This not only results in a reduction in the size of the contactor, but also the solvent circulation rate. The principle advantages of membrane gas–liquid contactors are operational flexibility, high mass transfer rate and easy linear scale-up. The operational flexibility is due to the absence of interpenetration of the phases in the contactor and hence the liquid and gas phase flowrates can be manipulated independent of each other, without any consequences like flooding, entrainment and weeping, as encountered in column type contactors. The absorption rate depends among others on the interfacial area for the gas–liquid contact (a) and mass transfer coefficient (k_L). The interfacial area for mass transfer in a membrane gas–liquid contactor is the membrane surface area. For commercially available hollow fiber membrane modules, it varies between 1500–3000 m^2/m^3 of contactor volume, depending on the diameter and packing density of the hollow fiber. This is much higher than the contact areas available in conventional contactors (100–800 m^2/m^3) like bubble columns, packed and plate columns (Westerterp, van Swaaij & Beenackers, 1984). In the membrane contactors, the high interfacial area is obtained at the cost of the fiber side mass transfer coefficient, which is low due to the laminar flow of fluids inside the fiber. Nevertheless, the volumetric mass transfer coefficient (k_La) is several times higher, resulting in a considerable reduction in the size of the contactor. Especially for offshore applications this offers tremendous advantages.

These unparalleled advantages over conventional column contactors seem to make the membrane modules an ideal gas–liquid contactor in the recovery/removal of CO_2 from flue gas, natural gas and different industrial process gas streams. Since the first pioneering work of Cussler and his coworkers (Qi & Cussler, 1985), there has been

* Corresponding author. Fax: +31-534-4894774.
E-mail address: g.f.versteeg@ct.utwente.nl (G. F. Versteeg).

0009-2509/02/$ - see front matter
PII: S0009-2509(02)00041-6

considerable academic and industrial research work done on this gas–liquid contactor concept for the removal of CO_2 (Gabelman & Hwang, 1999). However, only very few of these processes have been successfully tested on a larger scale. Kvaerner Oil & Gas and W.L. Gore & Associates GmbH have been developing a membrane gas absorption process for the removal of acid gases from natural gas and exhausts of the offshore gas turbines (Hanisch, 1999). In this process, PTFE hollow fiber membranes are used in combination with physical (Morphysorb®) or chemical solvents (alkanolamines). TNO Environment Energy and Process Innovation (The Netherlands) have been developing a membrane gas absorption process for the removal of CO_2 from flue gases using commercially available and cheaper polypropylene hollow fiber membranes. As conventional absorption liquids like alkanolamines are not suitable for polypropylene membranes, new reactive absorption liquids have been developed (Feron & Jansen, 1995).

Long-term stable operation of the membrane contactor requires that the pores of the membrane remain completely gas filled (non-wetted) over prolonged periods of operational time. This is because in case of wetted membranes, the gas to be absorbed also has to diffuse through the stagnant liquid inside the pores, thereby considerably increasing the overall mass transfer resistance. So, the prevention of wetting is an important criterion determining the operability of the contactor. Most of the absorption liquids used for the removal of gases like NH_3, SO_2, etc. are aqueous salt solutions and so membrane modules made of hydrophobic microporous membranes like polyolefin membranes were found to be ideally suitable. In case of reactive absorption of CO_2, conventional reactive absorption liquids like aqueous alkanolamine solutions were found to wet polyolefin membranes. However, many investigators had successfully used more hydrophobic membranes like Teflon (PTFE) to overcome wetting (Nishikawa et al., 1995). Unlike polypropylene hollow fibers, PTFE fibers are not available in small diameters (a few hundred microns) and they are more expensive, making CO_2 removal using membrane gas absorption (MGA) not so economically attractive in comparison to conventional absorption processes.

Thus, there is a need for the development of new absorption liquids for the removal of CO_2 using membrane contactors that can offer stable performance with relatively cheap polyolefin membrane. Also for oxygen rich gas streams like flue gas, it will be an added advantage if the new liquids have better thermal degradation properties than traditional alkanolamines. Amino acid salts can be a possible alternative to alkanolamines, though they are more expensive. The use of the salts of amino acids for acid gas removal has traditionally been restricted to using it as promoters for the conventional gas treating solvents (Kohl & Riesenfeld, 1995). Some of the noted amino acids used as promoters are glycine, alanine and diethyl or dimethyl glycine. TNO has developed and patented a range of absorption liquids based on amino acid salts and given them the trade name CORAL (CO_2 Removal Absorption liquid). These liquids offer similar absorption characteristics as aqueous alkanolamine solutions, have better degradation properties and above all, do not wet polypropylene membranes (Feron & Jansen, 1995). The present work deals with the above qualities of one such CORAL liquid as well as on the performance of this liquid in MGA, for the removal of CO_2. A numerical model involving mass transfer accompanied by multiple chemical reactions, occurring during the absorption of CO_2 into the absorption liquid flowing through the hollow fiber has been developed and the results of the numerical model have been compared with the experimental results.

2. Theory: mass transfer accompanied by chemical reactions

2.1. Reactive absorption of CO_2 in aqueous amino acid salt solutions

Amino acids dissolved in water exists as zwitter ion [form II in Eq. (1)] and the pH of the solution is equal to the isoelectric point of the given amino acid. The amino group should be deprotonated (form III) before it can react with CO_2. This is usually done by the addition of an equimolar amount of base.

$$\underset{\text{I}}{\text{HOOC}-\text{R}-\text{NH}_3^+} \overset{-\text{H}^+}{\rightleftharpoons} \underset{\text{II}}{{}^-\text{OOC}-\text{R}-\text{NH}_3^+} \overset{-\text{H}^+}{\rightleftharpoons} \underset{\text{III}}{{}^-\text{OOC}-\text{R}-\text{NH}_2}. \quad (1)$$

Aqueous solutions of amino acid salts react with CO_2 similar to primary alkanolamines. Unlike alkanolamines, there is no reliable information available in open literature regarding the reaction mechanism/kinetics and physico-chemical constants (such as physical solubility, diffusivity of CO_2 in aqueous salt solution) necessary to interpret the experimental kinetic data. In the present study, the potassium salt of taurine (2-aminoethanesulfonicacid) was used as a model amino acid salt and representative of the CORAL family of absorption liquids. To get reliable physico-chemical properties of the model component, several independent experimental studies were carried out (Kumar, Hogendoorn, Feron, & Versteeg, 2001a, b). The data were used in the present study, for the modeling of the absorption of CO_2 in the amino acid salt flowing through the hollow fiber (Section 2.2). The principle reactions occurring during the absorption of CO_2 in aqueous amino acid salt solutions are reaction (2) and (3) in the following scheme:

$$2\text{RNH}_2 + \text{CO}_2 \underset{k_{2,2}}{\overset{k_{2,1}}{\rightleftharpoons}} \text{RNHCOO}^- + \text{RNH}_3^+, \quad (2)$$

$$CO_2 + OH^- \underset{k_{3,2}}{\overset{k_{3,1}}{\rightleftharpoons}} HCO_3^-, \quad (3)$$

$$RNH_3^+ \underset{k_{4,2}}{\overset{k_{4,1}}{\rightleftharpoons}} RNH_2 + H^+, \quad (4)$$

$$H_2O \underset{k_{5,2}}{\overset{k_{5,1}}{\rightleftharpoons}} H^+ + OH^-. \quad (5)$$

Amino acid salts in aqueous solution react with CO_2, resulting in the formation of a carbamate and protonated amine. The mechanism of the reaction of CO_2 with the amino acid salts seems to be somewhat different from the well-known zwitterion mechanism proposed for the alkanolamines (Versteeg, van Dijck, & van Swaaij, 1996). The information on the forward reaction rate of the reaction (2) is given in the appendix. The contribution of reaction (3) to the overall reaction rate is usually not significant as the pH of the aqueous amino acid salt solutions is not high enough to have an appreciable concentration of OH^- ion in the liquid. Since the OH^- ion concentration is always in equilibrium with the amine concentration, the protonation/deprotonation (dissociation) reactions of the amino acid and water [given by reaction (4) and (5)] need to be considered also.

The experimental data on the physical solubility and diffusion coefficient of CO_2 in amino acid salt solutions were interpreted using appropriate mathematical models and are given in Appendix A. The kinetic, equilibrium and physico-chemical data related to the reactions (3)–(5) were obtained from the literature and they are also summarized in Appendix A. However, the experimental information on the equilibria of reaction (2) was only available for a narrow concentration range. The limited experimental data were regressed for the Kent–Eisenberg model and its value seems to be comparable to that of monoethanolamine (Kohl & Riesenfeld, 1995), the details of which are also given in Appendix A.

2.2. Numerical model

Numerous mass transfer models such as film, penetration and surface renewal models are available in literature to describe the reactive absorption of a gas in a liquid (Westerterp et al., 1984). The basic and common assumption of all these models is the presence of well-mixed bulk phase adjacent to the gas–liquid interface. For the present case of the reactive absorption of a gas in the liquid flowing through a hollow fiber, the well-mixed liquid bulk is absent. Due to the laminar flow of liquid through the hollow fiber, there is a velocity profile in the liquid phase, which extends from the gas–liquid interface to the axis of the fiber. Hence, the mathematical treatment of the present problem to predict the enhancement factor for the effect of chemical reaction on absorption is not easy. However, for physical absorption and constant gas–liquid interface conditions, Kreulen, Smolders, Versteeg, and van Swaaij (1993a) proposed an approximate solution for the mass transfer coefficient analogous to the heat transfer coefficient in the constant wall temperature heat transfer problem of Graetz (1883) and Leveque (1928) and it was experimentally validated.

$$Sh = \sqrt[3]{3.67^3 + 1.62^3 Gz}. \quad (6)$$

The above equation was found applicable for the complete range of Graetz numbers in the laminar flow regime. Due to the limitations mentioned above, the mass transfer process involving chemical reaction in the liquid flowing inside the hollow fiber has to be described by a model based on first principles. The differential mass balance for any species, i, present in the liquid phase is given by

$$v_z \frac{\partial C_i}{\partial z} = D_i \left[\frac{1}{r} \frac{\partial}{\partial r} \left(r \frac{\partial C_i}{\partial r} \right) \right] - R_i. \quad (7)$$

In arriving at Eq. (7), the diffusion in the axial direction was neglected and axi-symmetry was assumed. The temperature effect during the absorption process was considered to be negligible. As the liquid flow inside the fiber is laminar, the velocity profile in the radial direction is given by

$$v_z = 2v_L \left[1 - \left(\frac{r}{R} \right)^2 \right]. \quad (8)$$

The entrance effects had been neglected as the liquid flows through the hollow fiber for considerable distance ($> 100 d_{in}$, required for the velocity profile to be fully developed, see Perry & Green, 1984) before it contacts the gas phase. A generalized reversible reaction scheme to take into account the multiple reactions, as described in Section 2.1, was incorporated in the model. The partial differential equation (7) requires one initial condition and two boundary conditions in the axial and radial directions respectively. For the axial direction, the inlet conditions/properties of the liquid are specified.

$$\text{At } z = 0, \quad C_i = C_{i,0}. \quad (9)$$

In the radial direction, symmetry was assumed at the axis of the cylindrical fiber,

$$\text{At } r = 0, \quad \left(\frac{\partial C_i}{\partial r} \right) = 0. \quad (10)$$

At the gas–liquid interface, the conservation of mass with respect to the component that is absorbed from the gas phase (CO_2) was enforced.

$$\text{At } r = R \quad D_A \left(\frac{\partial C_A}{\partial r} \right) = k_{ext}(C_{A,g} - C_{A,g,i}). \quad (11)$$

All components other than the gas species absorbed are assumed to be non-volatile.

$$\text{At } r = R \quad \left(\frac{\partial C_i}{\partial r} \right) = 0 \quad \text{for } i \neq CO_2. \quad (12)$$

The set of partial differential equations (the number depending on the number of chemical species involved

in the reaction scheme) was solved numerically using a technique similar to the one described by Kreulen et al. (1993b). From the concentration profile of CO_2 in the liquid phase obtained from the solution of mass balance equations, the local absorption flux of CO_2 along the length of the fiber was calculated using Fick's law. The average CO_2 absorption flux ($\langle J_{CO_2} \rangle$) was obtained from integration of the local fluxes across the length of the fiber.

2.3. Analogy with conventional mass transfer models

Kumar et al. (2001c) showed that under limiting conditions, an analogy exists between the present mass transfer problem as described by Eq. (7) and conventional mass transfer models like the penetration model. For sufficiently short gas–liquid contact time in the hollow fiber, the penetration depth [approximately $0.5(D_A \pi L/v_L)^{0.5}$, see Westerterp et al., 1984] is a few orders of magnitude less than the radius of the hollow fiber (R). As a consequence, the liquid far away from the gas–liquid interface is unaffected by the absorption process. Physically this implies that the liquid is of infinite depth in comparison to the penetration depth of the gas. This is similar to the situation where a gas is absorbed in a falling film (of finite thickness and with constant velocity distribution in the liquid film) of a wetted wall column (Westerterp et al., 1984). For this limiting situation, the Hatta number (Ha^*) and infinite enhancement factor ($E^*_{i,\infty}$) can be defined on the properties of the liquid far away from the interface (at the axis of the fiber) analogous to the bulk liquid properties in conventional gas–liquid contactors. For an (1, 1)-order reaction, the dimensionless Hatta number and infinite enhancement factor can be defined as

Modified Hatta Number:

$$Ha^*_A = \sqrt{\frac{k_1 C_{B,\,r=0} D_A}{k_L}}. \tag{13}$$

Modified Infinite Enhancement Factor:

$$E_{a,\,\infty} = 1 + \frac{C_{B,\,r=0}}{v_B m C_{A,\,g,\,i}} \left(\frac{D_B}{D_A}\right)^{1/2}. \tag{14}$$

Here the mass transfer coefficient (k_L) can be calculated from Eq. (6). Developing an analogy with the conventional mass transfer models as described above, provides a convenient tool for the explanation of the experimental and numerical results in a simplistic way.

3. Experimental

3.1. Chemicals

The potassium salt of taurine was prepared by neutralizing taurine (Merck), dissolved in deionized water, with an equimolar amount of potassium hydroxide (Merck). The concentration of the amino acid salt was determined potentiometrically by titrating with standard HCl. Aqueous alkanolamine solutions used for comparison were prepared by dissolving pure alkanolamines (Merck) in deionized water. The concentration was determined by titrating with standard HCl.

3.2. Experimental setup and procedure

3.2.1. Surface tension and breakthrough pressure measurements

The wettability of a hydrophobic microporous membrane by a liquid depends, among others, on the surface tension of the liquid. It can be quantified by measuring the breakthrough pressure of the liquid through the membrane. The experimental technique to measure the breakthrough pressure was similar to the liquid entry pressure method described by Franken, Nolten, Mulder, Bargeman, and Smolders (1987). In this method, a dry membrane is brought into contact with a liquid after which the liquid pressure is increased. The pressure at which the liquid penetrates into the pores (this can be observed by the formation of the first liquid drop on the other side of the membrane) is measured. In the present study, the breakthrough pressure of various liquids was measured for a hydrophobic PTFE microporous membrane ($d_{p,\,\max}$: 3.5 μm; Schleicher & Schuell, Germany). The surface tension of the liquid was measured using two techniques: the Wilhelmy plate method (Kruss Digital Tensiometer K9, Kruss GmbH) and the maximum bubble pressure method (SITA Online t60, SITA Messtechnik GmbH). With the maximum bubble pressure method, the values of the surface tension were measured for a long bubble lifetime (60 s) inorder to obtain the equilibrium value of the surface tension. The values of the surface tension obtained with both methods were within ± 0.2 mN m^{-1}.

3.2.2. Absorption measurements

Absorption experiments were carried out in a single hollow fiber membrane contactor. Fig. 1 shows the single fiber contactor as well as the flowsheet of the experimental setup used for the absorption experiments. The contactor consisted of a jacketed, cylindrical glass tube with threaded ends as shown in Fig. 1. The two ends of a membrane hollow fiber were passed through two small stainless steel (SS) tubes whose inside diameter was slightly larger than the outside diameter of the hollow fiber. The length of the fiber exposed to the gas during absorption measurements was the distance between the two SS tubes. So, the distance between the SS tubes was carefully adjusted and the fiber was potted to the SS tubes on both the ends of the two tubes. The length of the fiber inside the SS tube (> 0.07 m), on the liquid entry side provides sufficient distance ($> 10 d_{in}$) for the laminar liquid flow inside the fiber to be fully developed, before it contacts the gas. The hollow fiber

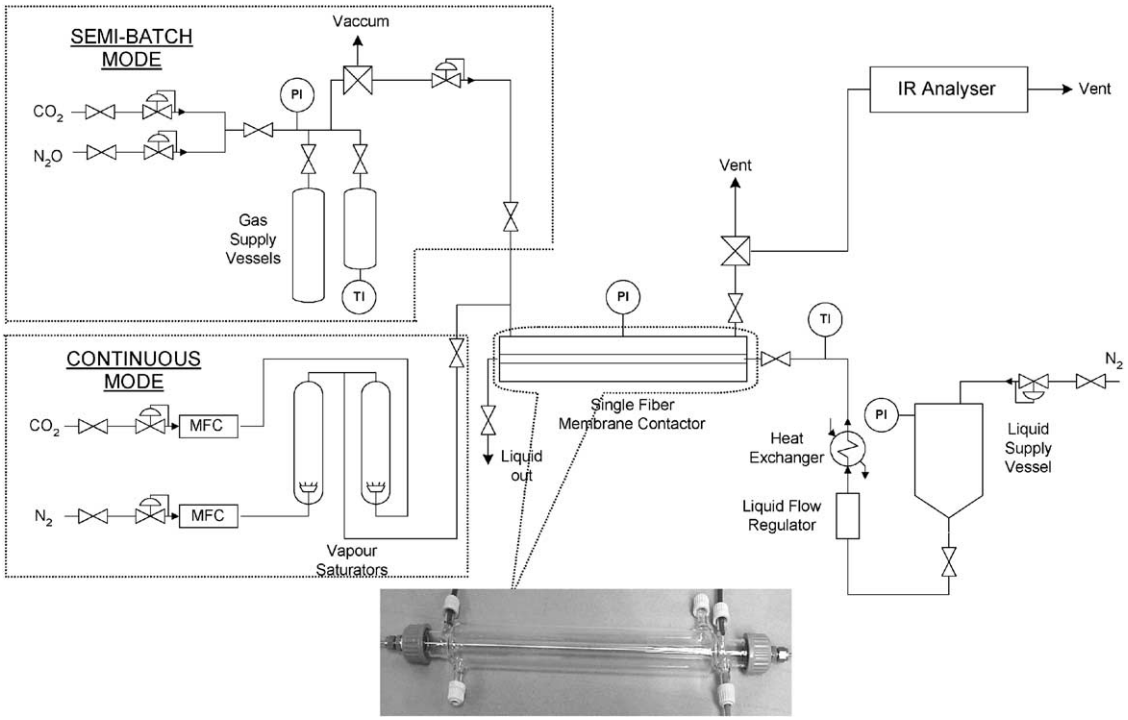

Fig. 1. Experimental setup to study the performance of new absorption liquids in a single fiber membrane gas–liquid contactor.

between the SS tubes was placed coaxial to the jacketed glass tube and the two SS tubes were fastened to the ends of the threaded glass tube (without stretching the fiber) with a special assembly as shown in the Fig. 1. The liquid feed line was connected to the SS tube on the feed side of the contactor.

Two modes of gas–liquid contacting operation were studied during the experiments. In both cases, the liquid flow through the fiber was continuous. The liquid was fed from a pressurized supply vessel to the membrane contactor via a flow controller. The inert gas (nitrogen) pressure above the liquid in the supply vessel was maintained constant using a precision pressure controller to enable a constant pulse-free flow of liquid through the fiber. The reactive liquids used in all the experiments were freshly prepared and degassed prior to the measurements. In the so-called semi-batch mode, the CO_2 partial pressure outside the hollow fiber in the contactor was maintained constant by feeding pure CO_2 from a gas supply vessel, through a pressure regulator. From the drop in the pressure of CO_2 in the gas supply vessel, the absorption rate and hence average CO_2 flux across the membrane was calculated. In case of the so-called continuous operation, nitrogen and CO_2 were premixed to a desired concentration using mass flow controllers and fed to the contactor after saturating the gas stream with water vapor. For all experiments studied, the gas flowed cocurrently with respect to the liquid phase. The CO_2 concentration in the feed and outlet gas streams of the contactor was measured using an Infrared analyzer. From this, the CO_2 absorption flux was estimated by making a mass balance over the reactor.

$$\langle J_{CO_2} \rangle = \frac{\phi_g (C_{A,\,g,\,\mathrm{in}} - C_{A,\,g,\,\mathrm{out}})}{d_{\mathrm{in}} L}. \tag{15}$$

It was assumed that the volumetric flowrate of the feed and exit streams are equal, as the concentration range of CO_2 in the feed stream studied was low (less than 6% by volume) and also, the fraction of the moles of CO_2 in the feed stream absorbed by the liquid was not high. For dilute gas streams flowing along the fiber, the contribution of the gas phase mass transfer resistance to the overall resistance can be significant. As the objective of the study is to understand the phenomenon of mass transfer with chemical reaction in the liquid phase, the gas phase resistance had to be minimized. The annular distance between the contactor glass wall and the outer surface of the fiber (through which the gas flows) was kept minimum and also the gas flowrate was increased till it had a negligible influence on the absorption rate. Absorption experiments were not conducted for high CO_2 concentrations in the gas stream, to avoid operating the contactor differentially (i.e., small concentration difference in the gas stream between inlet and outlet of the contactor). Differential operation can lead to large errors in the measurement of the absorption flux as the average flux is based on the inlet and outlet stream concentrations of CO_2 [Eq. (15)].

In the present work, the following systems were studied:

1. Physical absorption
   a. N_2O–water (semi-batch)
   b. CO_2–water (semi-batch)

2. Chemical absorption
   a. CO_2–NaOH(aq) (semi-batch)
   b. CO_2–amino acid salt(aq) (semi-batch & continuous).

The physical absorption experiments were studied to check the accuracy of the experimental setup for mass transfer measurements. Similarly, absorption of CO_2 in aqueous NaOH solution was chosen as a model reactive system, as accurate kinetic and physico-chemical data are available in literature. The hollow fiber membranes used for the experiments were supplied by Akzo Nobel (Accurel PP capillary membrane, Type Q3/2: average pore diameter: 0.2 μm; d_{in}: 600 μm).

4. Results and discussion

4.1. Wetting qualities of aqueous alkanolamines and amino acid salt solution for a hydrophobic microporous membrane

Wetting of the membrane depends on the properties of the liquid as well as the membrane material. These influences can be quantified in terms of surface tension of the liquid (γ_L), contact angle of the liquid with the membrane material (θ) and the pore properties of the membrane. A considerable amount of information is available in the literature on the criteria for wetting of microporous membranes (Franken et al., 1987). For low energy surfaces like polyolefin and PTFE, the relation between surface tension and contact angle is given by (Bargeman & van Voorst Vader, 1973)

$$\gamma_L \cos\theta = -\gamma_L + c. \tag{16}$$

For a single known value of γ_L and θ (usually for pure water), the constant c can be calculated. The influence of the presence of pores on the contact angle can be corrected as indicated by Troger, Lunktwitz and Burger (1997). With information on the values of surface tension, contact angle and pore properties, the minimum pressure to be applied on the liquid to enter the pores of the membrane (Breakthrough Pressure, BP) can be estimated using the Laplace–Young equation

$$\Delta p = -\frac{4\gamma_L \cos\theta}{d_{\max}}. \tag{17}$$

Here $d_{\max}$ is the maximum pore diameter in the microporous membrane. Table 1 shows experimental values of the surface tension of 2 molar primary, secondary and tertiary aqueous alkanolamine solutions measured at 295 ± 0.2 K. Aqueous solutions of alkanolamines are organic substances dissolved in water and their solubility is primarily due to the presence of the OH group. Hence their values of surface tension as shown in the table are significantly less than that of water. It can be observed that the surface tension progressively decreases from primary to tertiary amines or with increase in the molecular weight of the alkanolamines. Among tertiary amines, the surface tension of the aqueous MDEA solution is higher than that of the aqueous DMEA solution, due to the presence of an additional polar OH group in MDEA. For loaded solutions, the surface tension was found to increase with CO_2 loading and this can be explained by the presence of ionic reaction products formed during the reaction, of CO_2 with alkanolamines as given below (Versteeg et al., 1996).

For primary and secondary amines:

$$2RNH_2 + CO_2 \leftrightarrow RNHCOO^- + RNH3^+ \tag{18}$$

For tertiary amines:

$$R_3N + CO_2 + H_2O \leftrightarrow HCO_3^- + R_3NH^+. \tag{19}$$

The experimental breakthrough pressures for different loaded and unloaded aqueous alkanolamine solutions with a hydrophobic PTFE microporous membrane are shown in Table 1. These data are averaged values of at least five measurements with reproducibility within ±1 kPa. It should be noted that the maximum pore diameter of the PTFE membrane used ($d_{p,\max}$: 3.5 μm) was more than an order of magnitude higher than the pore diameter of the polypropylene membranes used in the actual absorption experiments (typically 0.2 μm). For polypropylene flat sheet membranes with a pore diameter of 0.2 μm, the breakthrough pressure for the liquids of high surface tension such as water and aqueous salt solutions are larger than the mechanical burst pressure of the membrane. Hence for a qualitative comparison of various alkanolamine solutions, a hydrophobic PTFE membrane with a larger pore diameter was used to measure the breakthrough pressure of all liquids having values of surface tension significantly higher (salts) and lower (amines) than that of water. As can be seen in Table 1, the influence of the type of amine and CO_2 loading on the breakthrough pressure follows exactly the same trend as observed for the surface tension.

Eventhough the value of the surface tension of an aqueous MEA solution is close to that of water, the breakthrough pressure for this liquid is significantly less than that of water, indicating possible changes in the surface/pore morphology of the membrane similar to the theory proposed by Barbe, Hogan, and Johnson (2000). Barbe et al. experimentally demonstrated for a hydrophobic membrane in contact with a liquid of low surface tension (also for water) that the pore equivalent diameter increases due to the non-wetting intrusion of the liquid meniscus into some pores with a resulting enlargement of the pore entrances. This enlargement of pores could result in wetting of the membranes at liquid pressures much lower than those predicted by Eq. (17). Fig. 2 shows the plot of experimental values of the breakthrough pressure measured for different

Table 1
Surface tension and breakthrough pressure of loaded and unloaded alkanolamine solutions at 295 K. The breakthrough pressure was measured for a PTFE membrane ($d_{p,\max}$: 3.5 μm, Schleicher & Schuell)

Alkanolamine	CO_2 loading (mol CO_2/mol amine)	γ_L (mN m^{-1})	Breakthrough pressure (kPa)
Water	Unloaded	72.3	25.4
Monoethanolamine (MEA)	Unloaded	68.2	18.2
Diethanolamine (DEA)	Unloaded	64.8	14.4
Methyldiethaolamine (MDEA)	Unloaded	57.2	13.1
Dimethylethanolamine (DMEA)	Unloaded	49.3	12.4
Monoethanolamine (MEA)	0.05	69.1	23.0
Monoethanolamine (MEA)	0.12	70.2	—
Monoethanolamine (MEA)	0.28	72.6	25.5

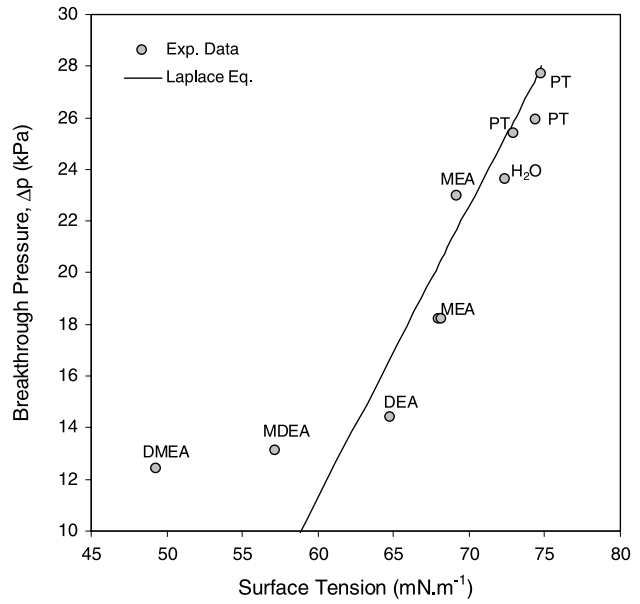

Fig. 2. Comparison of the experimental data of breakthrough pressure for a hydrophobic microporous PTFE membrane ($d_{p,\max}$: 3.5 μm, Schleicher & Schuell) with the values predicted by the Laplace–Young equation. The abbreviation 'PT' in the figure denotes potassium salt of taurine.

alkanolamine solutions. The line in the figure indicates the calculated value of breakthrough pressure using the Laplace–Young equation. Except for aqueous DMEA solution, the prediction of the Laplace–Young equation is reasonably good.

Table 2 gives some of the physical properties of unloaded and loaded aqueous amino acid salt solutions at 295 K. As expected, the surface tension of the aqueous amino acid salt solutions are higher than that for water. Unlike aqueous alkanolamines solutions, the surface tension increases with concentration of the salt and also increases with the CO_2 loading of the solution. Some experimental breakthrough pressure data of the aqueous amino acid salt solutions with a hydrophobic PTFE membrane are also shown in Fig. 2.

4.2. Absorption experiments

Experiments were carried out in semi-batch and continuous mode with respect to the gas phase. The semi-batch experiments were performed using pure CO_2, with the objective to test the experimental setup and also to generate experimental data to validate the numerical model for idealized and simple test conditions. The accuracy of the numerical model in comparison to the experimental data for the model amino acid salt studied indirectly gives an indication of the accuracy of the physico-chemical data (reaction kinetics, equilibrium solubility, diffusion coefficients, etc. see Appendix A and Kumar et al., 2001a, b), used as input parameters in the numerical model. The continuous mode of operation using dilute gas streams is of more practical relevance and therefore the concentration range of CO_2 removal from flue gas was simulated.

4.2.1. Physical absorption

Absorption of pure CO_2 and N_2O in degassed water was carried out in semi-batch mode. The results of the present experimental study are shown in Fig. 3, which shows that the numerical model accurately predicts the experimental data for both gases. The difference in the absorption flux for N_2O and CO_2 can primarily be accounted for by the difference in the physical solubility of these gases in water. To further investigate the accuracy of the numerical model, the length of the fiber was varied and absorption experiments were again carried out with pure CO_2. The influence of the fiber length is shown in Fig. 4 for different liquid velocities, which also shows a good agreement between theory and experiments. The accuracy of the liquid velocity in the experimental studies was within ± 0.005 m s^{-1}. It should be noted that for physical absorption, the influence of the length of the fiber on the absorption flux can also be theoretically quantified using the Graetz–Leveque solution [Eq. (6)]. The CO_2 absorption flux along the length of the fiber decreases due to saturation of the liquid by the gas and hence the average flux increases with decrease in length of the fiber exposed to gas.

Table 2
Physical properties of unloaded and loaded aqueous amino acid salt solutions at 295 K

Concentration (mol m^{-3}) $\times 10^{-3}$	CO_2 loading (mol CO_2/mol amine)	Viscosity (cP)	γ_L (mN m^{-1})	Breakthrough pressure (kPa)
1.0	Unloaded	1.18	72.9	25.4
2.0	Unloaded	1.59	74.4	25.9
4.0	Unloaded	3.27	77.5	—
2.0	0.04	—	74.8	27.7
2.0	0.17	—	75.3	—
2.0	0.32	—	76.1	—

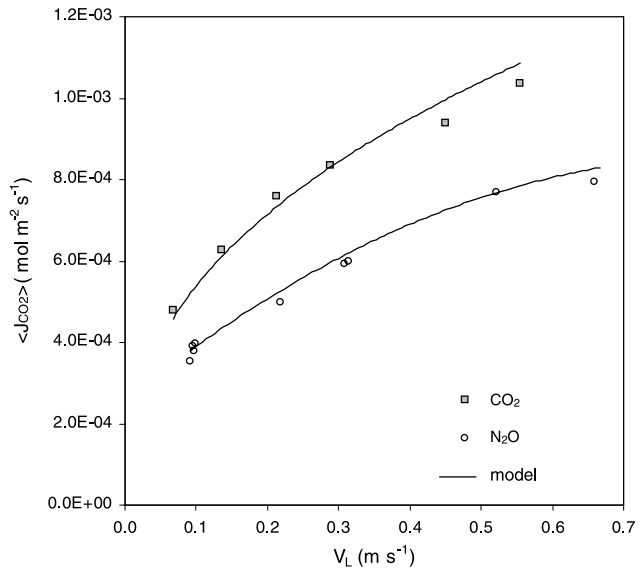

Fig. 3. Physical absorption of CO_2 and N_2O in water flowing through a hollow fiber. (Semi-batch; L: 0.38 m; P_{gas}: 107 kPa; T: 295 K.)

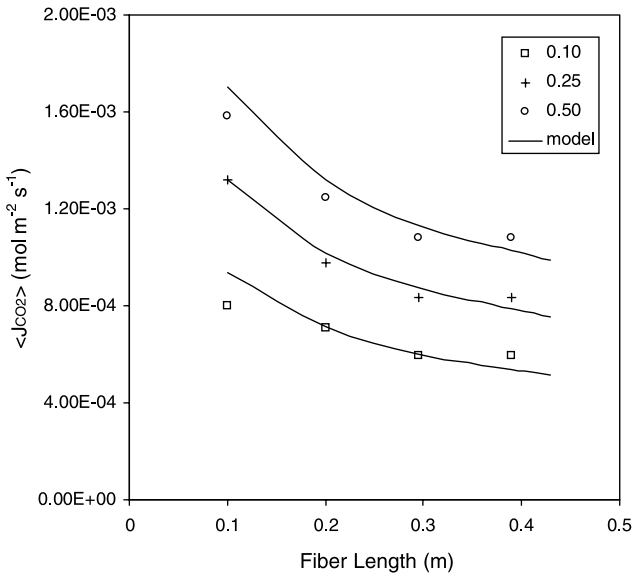

Fig. 4. Influence of fiber length on the absorption rate of CO_2 in water flowing through the hollow fiber. The legend of the figure indicates the liquid velocity in m s^{-1}. (Semi-batch; T: 293 K; P_{gas}: 107 kPa.)

4.2.2. *Absorption enhanced by chemical reaction*

4.2.2.1. *Absorption of* CO_2 *in aqueous NaOH solution*

Absorption of CO_2 in aqueous NaOH is widely used as a model system to investigate the performance of gas–liquid contactors. As the surface tension of these liquids is high (due to their ionic nature), they do not wet polyolefin microporous membranes. Considerable and accurate information is available in the literature on the physico-chemical parameters required to model the absorption process. So, this system was used as a model system to study absorption enhanced by chemical reaction in a hollow fiber. In the numerical model only reaction (3) was considered for the simulations. The kinetic, solubility and diffusivity data used as input parameters in the model were obtained from literature (Pohorecki & Moniuk, 1988; Schumpe, 1993; Hikita, Asai, & Takatsuka, 1972). Electroneutrality in the liquid phase was maintained by using mean ion diffusion coefficients for the ionic species in the liquid phase. The results of the experimental study as well as that of the model are shown in Fig. 5. It can be seen that the model predictions are in good agreement with experimental results.

4.2.2.2. *Absorption of* CO_2 *in aqueous amino acid salt solutions Influence of liquid velocity.*

Liquid velocity is perhaps the most important operating variable in the membrane gas–liquid contactors because in general it has a large influence on the absorption flux. Depending on the liquid velocity (and hence Ha^*) and $E^*_{a,\infty}$, the absorption regime continuously changes from the liquid entrance to the exit. At the liquid inlet, there is no depletion of the amine at the gas–liquid interface and the absorption rate is influenced by the chemical reaction rate (kinetics), while the liquid velocity has no effect on the local absorption rate (Fast regime; $Ea = Ha^*$). Further, along the length of the fiber (depending on Ha^* and $E^*_{a,\infty}$), depletion of the amine may occur at the interface. For the extreme case of complete depletion of amine at the interface, the absorption rate is limited by the radial diffusion of the reacting species to the reaction plane and the flux is strongly influenced by the mass transfer coefficient (instantaneous regime; $Ea = E^*_{a,\infty}$).

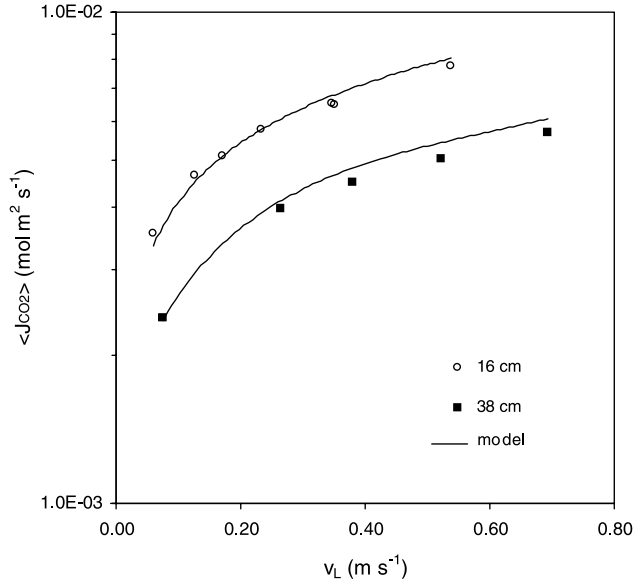

Fig. 5. Influence of liquid velocity on the absorption rate of CO_2 in aqueous NaOH solutions flowing through a hollow fiber. The numbers in the legend of the figure indicate the length of the fiber. (Semi-batch; C_{NaOH}: 0.24 M; P_{gas}: 107 kPa; T: 295 K.)

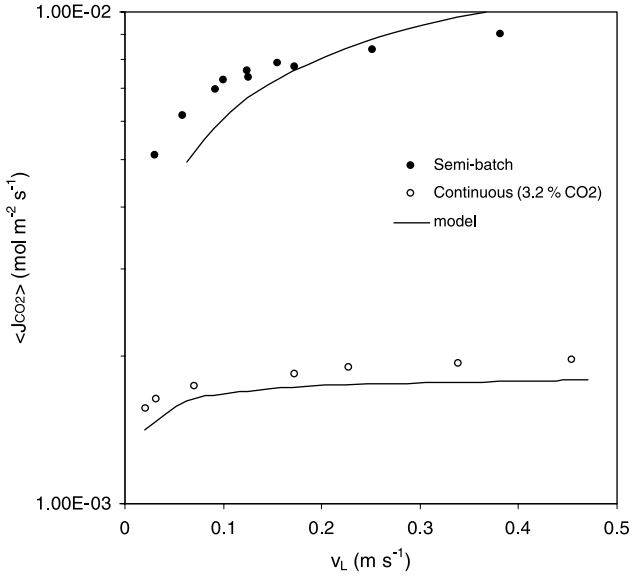

Fig. 7. Influence of liquid velocity on the absorption rate of CO_2 in aqueous amino acid salt solution flowing through the hollow fiber. (L: 0.426 m; C_{AmA}: 0.992 M; $P_{gas,\ s.batch}$: 107 kPa; $P_{gas,\ cont}$: 103 kPa; T: 295 K.)

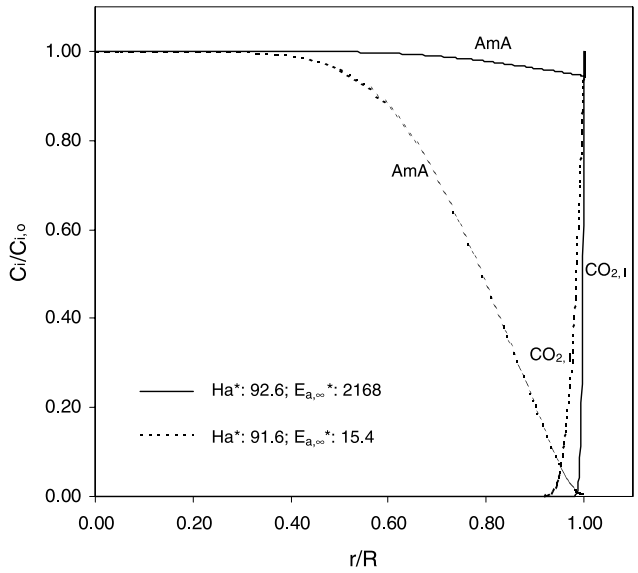

Fig. 6. The numerical radial concentration profile of the amino acid salt and CO_2 in the liquid phase during the absorption of CO_2 in the amino acid salt solution flowing through the fiber, for two asymptotic absorption regimes, namely fast ($2 < Ha^* < E_{a,\infty}$) and instantaneous ($2\langle Ha^*\rangle E_{a,\infty}$). The radial profile is at the liquid exit of the fiber (i.e., $z = L$). (L: 0.165 m; R: 300 μm, v_L: 0.10 m s^{-1}; $C_{AmA,o}$: 992 mol m^{-3}; P_{CO_2}: 107 kPa for instantaneous regime and 0.77 kPa for fast regime; T: 295 K.)

As an example, Fig. 6 shows the numerically calculated radial concentration profiles of the amino acid salt and CO_2 in the liquid phase at the liquid exit of the fiber ($z = L$). The experimental conditions for which the simulations were carried out are given in the figure. It can be clearly observed that there is no significant depletion of the amino acid salt for $2 < Ha^* < E^*_{a,\infty}$ (fast regime). In the present study, the partial pressure of CO_2 in the gas stream is low and therefore the absorption in the continuous experiments fulfilled this condition. However for the case $2\langle Ha^*\rangle E^*_{a,\infty}$, the concentration of the amino acid salt at the gas–liquid interface approaches zero and a reaction plane is formed. This situation is analogous to the instantaneous regime described by the conventional mass transfer models. This example shows that the conventional mass transfer models can be used to describe the absorption of a gas in a liquid flowing through the hollow fiber. The necessary condition for the use of the conventional mass transfer model is that the gas–liquid contact time (residence time of the liquid) should be short enough to prevent the depletion of the amino acid salt at the axis of the fiber.

Fig. 7 shows the influence of the liquid velocity on the absorption rate of CO_2 from a gas phase, for two different partial pressures of CO_2. The numerical model predicts the experimental trend and data reasonably well. For the semi-batch experiments, where pure CO_2 is used, the absorption regime in a part of the fiber is instantaneous and hence absorption rate is influenced by the liquid velocity. During absorption from a gas stream containing a low partial pressure of CO_2, except at very low liquid velocity, the absorption rate is not influenced by v_L significantly. So, at a liquid velocity above few centimeters per second, the absorption regime is in the $Ea = Ha^*$ regime and this regime is ideally suitable for the operation of the membrane contactor.

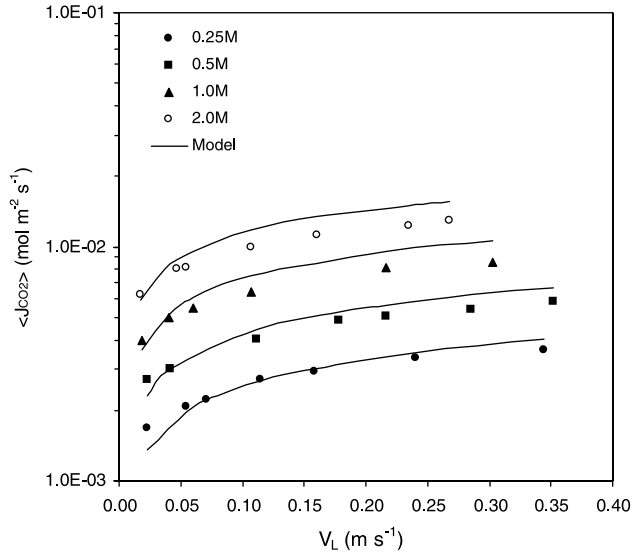

Fig. 8. Influence of amino acid salt concentration on the absorption rate of CO_2 in the semi-batch measurements. The legends in the figure indicate the molar concentration of the solution used (L: 0.165 m; P_{gas}: 107 kPa; T: 295 K.)

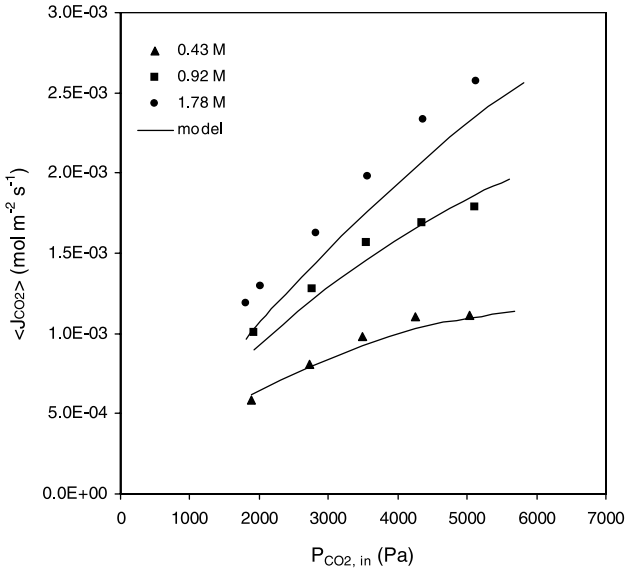

Fig. 9. Influence of the partial pressure of CO_2 in the feed gas stream on the absorption rate of CO_2 in aqueous amino acid salt solution flowing through the hollow fiber membrane. The legends in the figure indicate the molar concentration of the salt in liquid. (Continuous; L: 0.38 m; v_L: 0.025 m s^{-1}; $P_{gas.}$: 103 kPa; T: 295 K.)

Influence of amino acid salt concentration and partial pressure of CO_2 (*semi-batch and continuous experiments*).

Absorption of pure CO_2 in aqueous amino acid salt solutions of different concentrations was investigated and the results are shown in Fig. 8. For a CO_2 partial pressure of approximately 100 kPa in the gas phase and low amine concentration in the liquid phase, there is a significant depletion of the amine at the gas–liquid interface (indicating the instantaneous absorption regime) and hence the liquid velocity (i.e., k_L) significantly influences the absorption flux, as described earlier. As it can be seen in Fig. 8, the numerical model predicts the experimental data within $\pm 20\%$. The lower accuracy in the prediction of the numerical model in comparison to the aqueous NaOH–CO_2 system can be partly due to the inaccuracy in the values of equilibrium constants used in simulations for reaction (2).

Fig. 9 shows the influence of the partial pressure of CO_2 in the feed gas stream for different amino acid salt concentrations in the liquid stream. For a given salt concentration, the flux increases linearly with the partial pressure of CO_2 in the feed stream and it is strongly dependent on the amino acid salt concentration. The experimental absorption flux is nearly proportional to $C_{AmA}^{n/2}$ (which is in accordance with the power in the Hatta number), where n is the order of the reaction with respect to the amino acid salt. Also, at these operating conditions (except for a 0.43 molar solution), the absorption was not significantly affected by the liquid velocity (see also Fig. 7) and thus independent of k_L. Combining together these observations, it can be concluded that for those conditions the absorption rate is principally influenced by the reaction kinetics and there is no significant depletion of the amine at the gas–liquid interface ($Ea = Ha^*$). The numerical model predicts the experimental data within $\pm 25\%$.

As the stability of a membrane contactor is of paramount importance, additionally the CO_2 absorption flux was monitored in the single fiber reactor for 72 h for a 2 molar amino acid salt solution. During this prolonged period of operation, the flux dropped by only 6% and this drop was mainly observed during the initial period of 30 min.

5. Conclusions

In the present study, a new absorption liquid based on the alkaline salts of amino acids was studied in an experimental, single fiber membrane gas–liquid contactor. The new liquid has suitable physical properties to prevent the wetting of commercially available polypropylene microporous membranes and also has good reactivity towards CO_2. The liquids based on amino acid salts seem promising for the removal of CO_2 in membrane contactors and are suited for stable gas–liquid contacting.

The wetting of the microporous membranes was studied by measuring the breakthrough pressure of the liquid for a hydrophobic membrane. Experimental results of the breakthrough pressure and surface tension for different classes of aqueous alkanolamines and amino acid salt solutions explain qualitatively the underlying reason for the wetting of polyolefin membranes by alkanolamines and also, the opposite

phenomenon encountered for amino acid salts. The Laplace–Young equation could be conveniently used to predict the breakthrough pressure of various liquids for a microporous membrane.

Membrane gas absorption experiments were performed extensively to determine the performance of the non-wetting aqueous amino acid salt solutions in the removal of CO_2 from dilute gas streams. Absorption of CO_2/N_2O in water and aqueous NaOH solutions were used as model non-reactive and reactive experimental systems, respectively, to establish the accuracy of the experimental setup and the applicability of the numerical model. Under limiting conditions, the experimental trends of the absorption flux with respect to the various operating parameters can be conveniently explained using traditional mass transfer models.

A numerical model has been developed to simulate mass transfer accompanied by multiple chemical reactions, occurring during the absorption of a gas in the liquid flowing through the hollow fiber. The numerical model provides good insights on the mass transfer process occurring in the liquid phase flowing through the fiber and it accurately predicts the experimental data of model reactive and non-reactive systems. For the absorption of CO_2 in aqueous amino acid salt solutions, the experimental data are predicted within $\pm 25\%$ for a wide range of experimental conditions.

Notation

c	constant in Eq. (16), mN m^{-1}
C	concentration, mol m^{-3}
d_{in}	inside diameter of the hollow fiber, m
$d_{p,\,\max}$	maximum pore diameter, μm
D	diffusion coefficient, m^2 s^{-1}
$d_{\max}$	maximum pore size, m
Ea	enhancement factor, dimensionless
$E_{a,\,\infty}$	modified infinite enhancement factor, dimensionless
F	Faradays constant, C mol^{-1}
Gz	Graetz number, $v_L d^2/DL$, dimensionless
Ha^*	modified Hatta number, dimensionless
h_I	ion specific constant, m^3 kmol^{-1}
h_G	gas specific constant, m^3 kmol^{-1}
h_-	anion specific constant, m^3 kmol^{-1}
h_I	cation specific constant, m^3 kmol^{-1}
$\langle J_{CO_2} \rangle$	average CO_2 absorption flux, mol m^{-2} s^{-1}
K_{sub}	reaction equilibrium constant, sub: reaction number, $k_{\text{subs},\,1}/k_{\text{sub},\,2}$
$k_{\text{sub},\,1}$	reaction rate constant, sub: reaction number, 1: forward, (mol^{-1} m^3)^n s^{-1}
$k_{\text{sub},\,2}$	reaction rate constant, sub: reaction number, 2: backward, (mol^{-1} m^3)^n s^{-1}
k_{ext}	external mass transfer coefficient, m s^{-1}
k_L	liquid side mass transfer coefficient, m s^{-1}
L	length of the hollow fiber, m
m	physical solubility, $(C_{A,\,l}/C_{A,\,g})_{\text{eq}}$, dimensionless
n	overall order of the reaction, dimensionless
P_{gas}	pressure in the gas phase, kPa
r	distance in radial direction from the fiber axis, m
R	radius of the fiber, m
R_i	reaction rate, mol m^{-3} s^{-1}
Sh	Sherwood number, $k_L d/D$, dimensionless
T	temperature, K
v_L	average liquid velocity, m s^{-1}
v_z	liquid velocity in the axial direction, m s^{-1}
z	distance in the axial direction from the liquid inlet, m
z^+, z^-	ionic charge

Greek letters

γ_L	surface tension of liquid, mN m^{-1}
Δp	breakthrough pressure, kPa
θ	contact angle of the liquid with solid surface
λ^∞	ionic conductivity at infinite dilution, m^2 Ω^{-1} mol^{-1}
μ	liquid viscosity, kg m^{-1} s^{-1}
v	stoichiometric coefficient
ϕ	gas flowrate, m^3 s^{-1}

Subscripts

∞	infinite dilution
A	component in gas phase
AmA	amino acid salt
B	component in liquid phase
g	gas phase
l	liquid phase
i	component i, interface
in	feed stream
out	outlet stream
o	inlet condition
s	salt
w	water

Superscripts

∞	infinite dilution
$+, -$	charge of the ion

Abbreviations

BP	breakthrough pressure
DEA	diethanolamine
DMEA	dimethylethanolamine
MDEA	methyldiethanolamine
MEA	monoethanolamine
MGA	membrane gas absorption
PT	potassium taurate
PTFE	polytertraflouroethylene

Acknowledgements

This research is part of the research programme carried out within the Centre for Separation Technology, a cooperation between the University of Twente and TNO, the Netherlands Organisation for Applied Scientific Research. We also acknowledge L. H. Laagwater for his assistance to the experimental work and Wim Leppink for the construction of experimental setups.

Appendix A.

The physical and chemical parameters for CO_2-aqueous amino acid salt system were obtained from independent experimental studies. Part of these studies have been published in the open literature (Kumar et al., 2001b) and others will be published shortly hereafter (Kumar et al., 2001a).

A.1. Physical solubility

As CO_2 reacts with the aqueous amino acid salt solutions, the physical solubility of CO_2 in the salt solutions was indirectly obtained from the solubility of N_2O. A model similar to that of Schumpe (1993) described the experimental data on the solubility of N_2O in aqueous potassium taurate solutions (Kumar et al., 2001b).

$$\log(m_w/m) = KC_s,$$

where C_s is the salt concentration in mol m^{-3}. For a single salt, the Sechenov constant, K based on the Schumpe model is given by the following relation:

$$K = \sum (h_i + h_G) n_I \quad \text{m}^3\ \text{kmol}^{-1}.$$

The anion and cation specific constants are:

h_+: 0.0922 m^3 $kmol^{-1}$,

h_-: 0.0249 m^3 $kmol^{-1}$.

The temperature dependent gas (CO_2) specific constant was obtained from the database of Schumpe (1993). The solubility of CO_2 and N_2O in water (m_w) were obtained from the work of Versteeg and van Swaaij (1988)

A.2. Diffusion coefficient

An approach similar to the physical solubility was used to determine the diffusivity of CO_2 in aqueous salt solutions. The diffusion coefficient of N_2O in potassium taurate solution was obtained from Kumar et al. (2001b). A modified Stokes–Einstein equation was used for the estimation of the diffusion coefficient of N_2O in aqueous potassium taurate solutions.

$$D\mu^{0.74} = \text{constant}.$$

The information on the dependence of viscosity on the amino acid salt concentration is available in Kumar et al. (2001b). The diffusion coefficient of CO_2 in aqueous potassium taurate solutions was estimated according to Gubbins, Bhatia, and Walker (1966):

$$(D/D_w)_{N_2O} = (D/D_w)_{CO_2}.$$

The diffusion coefficients of CO_2 and N_2O in water were obtained from the work of Versteeg and van Swaaij (1989).

The mean ion diffusion coefficient of the amino acid salt in aqueous solution, at infinite dilution was estimated using the Nernst equation (Hovarth, 1985).

$$D_i^{\infty} = \frac{z^+ + z^-}{z^+ z^+} \frac{RT}{F^2} \frac{\lambda_+^{\infty} \lambda_-^{\infty}}{\lambda_+^{\infty} + \lambda_-^{\infty}}.$$

The ionic conductivity at infinite dilution for the potassium ion (λ_+^{∞}) was fitted as a polynomial function of temperature from the data available in Hovarth (1985). Similarly λ_-^{∞} for the anion was obtained for 298 K from Greenstein and Winitz (1961). As information on the temperature dependence of λ_-^{∞} was not available in the literature for the taurate ion, the dependence was assumed to be similar to that of the cation. At 295 K, the values of λ_+^{∞} and λ_-^{∞} are 70.1 and 28.9 $m^2\ \Omega^{-1}\ mol^{-1}$, respectively. The dependence of the diffusion coefficient of the amino acid salt in aqueous solution on the salt concentration was assumed to follow the modified Stokes–Einstein relation (Versteeg et al., 1996):

$$D\mu^{0.6} = \text{constant}.$$

Diffusivities of protonated amine and carbamate were estimated from the amino acid salt diffusivities as no data are available in literature.

A.3. Kinetics and equilibria parameters

The forward reaction rate of the reaction between CO_2 and aqueous potassium taurate solution was obtained from Kumar et al. (2001a) and is given by the following relation:

$$R_{CO_2} = \frac{k_2[CO_2][Am]}{1 + \frac{1}{k_{AmA}[AmA] + k_{H_2O}[H_2O]}} \quad \text{mol m}^{-3}\ \text{s}^{-1}.$$

Here C_{Am}, C_{H_2O} and $C_{CO_2,l}$ are the concentration of amino acid salt, water and carbon dioxide in the absorption liquid respectively in mol m^{-3}. The temperature dependency of k_2 is given by an Arrhenius type relation. However, k_{AmA} and k_{H_2O} are temperature independent.

$$k_2 = 2.809 \times 10^{-7} \exp\left(-\frac{5700}{T}\right) \quad \text{m}^3\ \text{mol}^{-1}\ \text{s}^{-1},$$

$$k_{H_2O} = 1.149 \times 10^{3} \exp\left(\frac{1483}{T}\right) \quad \text{m}^3\ \text{mol}^{-1},$$

$$k_{AmA} = 1.634 \times 10^{4} \exp\left(\frac{1225}{T}\right) \quad \text{m}^3\ \text{mol}^{-1}.$$

The forward rate constant of reaction (3) as a function of ionic strength, I (mol m^{-3}) was obtained from Pohorecki and Moniuk (1988).

$$\log(k_{3,1}/k_{3,1}^{\infty}) = 2.21 \times 10^{-4} I - 1.6 \times 10^{-8} I^2$$

and the rate constant at infinite dilution is given by

$$k_{3,1}^{\infty} = 8.895 - (2382/T) \quad \mathrm{m^3\ mol^{-1}\ s^{-1}}.$$

As the reactions (4) and (5) were instantaneous, a large value of forward rate constant (10^6 m^3 mol^{-1} s^{-1}) was used for $k_{4,1}$ and $k_{5,1}$.

The backward reaction rates were estimated by the assumption that at equilibrium conditions, forward and backward rates are equal. The equilibrium constant of reaction (2) was obtained from regression of limited experimental data for the Kent–Eisenberg model (Kohl & Riesenfeld, 1995) and the value is given below. Further experimental work on the equilibria is currently in progress.

$$K_2 = (C_{\mathrm{RNHCOO^-}} C_{\mathrm{RNH_3^+}})/(C_{\mathrm{RNH_2}}^2 C_{\mathrm{CO_2},l})$$

$$= 2.64 \times 10^5 \quad (\mathrm{m^3\ kmol^{-1}}).$$

The equilibrium constant (K_3) of reaction (3) was obtained from Edwards et al. (1978). Similarly, the dissociation (equilibrium) constants of amino acid (K_4) and water (K_5) were obtained from Perrin (1965) and Edwards, Maurer, Newman, and Prausnitz (1978), respectively.

References

Barbe, A. M., Hogan, P. A., & Johnson, R. A. (2000). Surface morphology changes during initial usage of hydrophobic, microporous polypropylene membranes. *Journal of Membrane Science*, *172*, 149–156.

Bargeman, D., & van Voorst Vader, F. (1973). Effect of surfactant on contact angles at non-polar solids. *Journal of Colloid and Interface Science*, *42*(3), 467–472.

Edwards, T. J., Maurer, G., Newman, J., & Prausnitz, J. M. (1978). Vapour-liquids equilibria in multicomponent aqueous solutions of volatile weak electrolytes. *A.I.Ch.E. Journal*, *24*, 966–976.

Feron, P. H. M., & Jansen, A. E. (1995). Capture of carbon-dioxide using membrane gas-absorption and reuse in the horticultural industry. *Energy Conversion and Management*, *36*(6–9), 411–414.

Franken, A. C. M., Nolten, J. A. M., Mulder, M. H. V., Bargeman, D., & Smolders, C. A. (1987). Wetting criteria for the applicability of membrane distillation. *Journal of Membrane Science*, *33*, 315–328.

Gabelman, A., & Hwang, S. T. (1999). Hollow fiber membrane contactors. *Journal of Membrane Science*, *159*(1–2), 61–106.

Graetz, L. (1883). Über die Wärmeleitungsfähigkeit von Flüssigkeiten, 1e Abhandlung. *Annalen der Physik und Chemie*, *18*, 79–84.

Greenstein, J. P., & Winitz, M. (1961). *Chemistry of the amino acids*. New York: Wiley.

Gubbins, K. E., Bhatia, K. K., & Walker, R. D. (1966). Diffusion of gases in electrolytic solutions. *A.I.Ch.E. Journal*, *12*, 548–552.

Hanisch, C. (1999). Exploring options for CO_2 capture and management. *Environmental Science and Technology*, *33*(3), 66A–70A.

Hikita, H., Asai, S., & Takatsuka, T. (1972). Gas absorption with a two step chemical reaction. *Chemical Engineering Journal*, *4*, 31–40.

Hovarth, A. L. (1985). *Handbook of aqueous electrolytic solutions: physical properties, estimation and correlation methods*. New York: Wiley.

Kohl, A. L., & Riesenfeld, F. C. (1995). *Gas purification* (5th ed.). Houston: Gulf Publishing Company.

Kreulen, H., Smolders, C. A., Versteeg, G. F., & van Swaaij, W. P. M. (1993a). Microporous hollow-fiber membrane modules as gas–liquid contactors. 1. Physical mass transfer processes — A specific application — Mass transfer in highly viscous liquids. *Journal of Membrane Science*, *78*(3), 197–216.

Kreulen, H., Smolders, C. A., Versteeg, G. F., & van Swaaij, W. P. M. (1993b). Microporous hollow-fiber membrane modules as gas–liquid contactors. 2. Mass transfer with chemical reaction. *Journal of Membrane Science*, *78*(3), 217–238.

Kumar, P. S., Hogendoorn, J. A., Feron, P. H. M., & Versteeg, G. F. (2001a). On kinetics of reaction between CO_2 and aqueous amino acid salt solutions, to be published.

Kumar, P. S., Hogendoorn, J. A., Feron, P. H. M., & Versteeg, G. F. (2001b). Density, viscosity, solubility and diffusivity of N_2O in aqueous amino acid salt solutions. *Journal of Chemical and Engineering Data*, *46*, 1357–1361.

Kumar, P. S., Hogendoorn, J. A., Feron, P. H. M., & Versteeg, G. F. (2001c). Approximation solutions to estimate enhancement factor during reactive absorption of a gas in the liquid flowing inside a microporous hollow fiber, to be published.

Leveque, J. (1928). Les lois de la transmission de chaleur par convection. *Annls of Mines*, Paris (12), 201.

Nishikawa, N., Ishibashi, M., Ohta, H., Akutsu, N., Matsumoto, H., Kamata, T., & Kitamura, H. (1995). CO_2 Removal by hollow-fiber gas–liquid contactor. *Energy Conversion and Management*, *36*(6–9), 414–418.

Perrin, D. D. (1965). *Dissociation of organic bases in aqueous solution*. London: Butterworth.

Perry, R. H., & Green, D. (1984). *Perry's chemical engineer's handbook*. Singapore: McGraw-Hill.

Pohorecki, R., & Moniuk, W. (1988). Kinetics of the reaction between carbon dioxide and hydroxyl ion in aqueous electrolyte solutions. *Chemical Engineering Science*, *43*, 1677–1684.

Qi, Z., & Cussler, E. L. (1985). Microporous hollow fibers for gas absorption I. Mass transfer in the liquid. *Journal of Membrane Science*, *23*, 321–333.

Schumpe, A. (1993). The estimation of gas solubilities in salt solutions. *Chemical Engineering Science*, *48*, 153–158.

Troger, J., Lunktwitz, K., & Burger, W. (1997). Determination of the surface tension of microporous membrane using contact angle measurements. *Journal of Colloid and Interface Science*, *194*(2), 281–286.

Versteeg, G. F., van Dijck, L. A. J., & van Swaaij, W. P. M. (1996). On the kinetics between CO_2 and alkanolamines both in aqueous and non-aqueous solutions. An overview. *Chemical Engineering Communications*, *144*, 113–158.

Versteeg, G. F., & van Swaaij, W. P. M. (1988). Solubility and diffusivity of acid gases (CO_2, N_2O) in aqueous alkanolamine solutions. *Journal of Chemical and Engineering Data*, *33*, 29–34.

Westerterp, K. R., van Swaaij, W. P. M., & Beenackers, A. A. C. M. (1984). *Chemical reactor design and operation*. New York: Wiley.